Talanta 81 (2010) 1250–1257

Contents lists available at ScienceDirect

Talanta

journal homepage: www.elsevier.com/locate/talanta

Effect of the size of electrode on electrochemical properties of ferrocene-functionalized polypyrrole towards DNA sensing

H.Q.A. Lê[a], S. Chebil[a], B. Makrouf[b], H. Sauriat-Dorizon[b], B. Mandrand[b], H. Korri-Youssoufi[a,*]

[a] Equipe de Chimie Bioorganique et Bioinorganique, CNRS UMR 8182, Institut de Chimie Moléculaire et de Matériaux d'Orsay, Université Paris-Sud, Bâtiment 420, 91405 Orsay, France
[b] bioMérieux, Interface Chemistry Research and Development, Engineering and System Dpt Chemin de l'Orme, Marcy l'Etoile, 69280, France

ARTICLE INFO

Article history:
Received 17 September 2009
Received in revised form 3 February 2010
Accepted 7 February 2010
Available online 16 February 2010

Keywords:
Biosensors
Biochips
DNA hybridization
Electrochemical detection
Polypyrrole
Ferrocenyl groups

ABSTRACT

A simple and highly sensitive electrochemical DNA sensor based on a ferrocene-functionalized polypyrrole has been prepared on a microelectrode array substrate for a multi-DNA detection chip format. A copolymer formed with 1-(phthalimidylbutanoate)-1′-(N-(3-butylpyrrole)butanamide)ferrocene (Py-Fe-NHP) and pyrrole was electrocopolymerized on the gold surface of both macroelectrode and biochip formats. DNA probes bearing an amino group were covalently grafted by substitution of NHP groups and the hybridization reaction was followed by monitoring the redox signal of the ferrocenyl group acting as the probe. The integration of the polymers into chip format produces high-density arrays of individually addressable oligonucleotide microelectrodes. Results show that reducing the size of the electrodes from a macroelectrode to the chip format allows a variation of the nucleation and the growth process during electropolymerization of modified pyrrole monomers. These modifications enable an increase in the sensitivity and selectivity of DNA hybridization.

1. Introduction

The detection of DNA sequences is of particular interest in genetics, pathology, pharmacogenetics, food analysis and many other fields. Multiplexed DNA analysis is usually performed using microarray technology which provides analytical devices that allows the parallel and simultaneous detection of several thousands of probes within one sample [1]. Currently, most DNA microarrays use optical biosensing based on a fluorescent dye marker for detection, which requires many processes of analysis before detection. Direct detection techniques without labelling, combined with DNA microarray format, remain under development. For this purpose, electrochemical methods are attractive because they are amenable to direct electrical readout, and are also well suited for rapid detection with high sensitivity and selectivity with low-cost instrumentation and adaptable to miniaturization [2]. Various methods for the immobilization of DNA have been developed in order to reach the necessary high density on a small surface. For example, conducting polymers (CPs) have been shown to be versatile substrates for the elaboration of DNA biosensor microarrays [3]. The main advantage lies on the ability to control the electrically deposition which is compatible with microarray chip format [4]. In addition, the perturbations in the polymer chain caused by the presence of the probe/target interaction leads to a change in macroscopic material properties [5] such as conductivity [6], redox activity [7–10] or optical properties [11]. However, applications of CP biosensors on DNA chips need real improvement in their sensitivity before the promise of commercial devices can be achieved. To address the problem associated with using solely the CP as the probe system, a combined CP and redox probe acting as an electrochemical ODN sensor based on a polypyrrole multi-functionalized with ferrocenyl groups and DNA probe have been previously developed [12,13]. The rationale behind its design is as follows: the ferrocenyl group is known to have a reversible and narrow electrochemical signal which is sensitive to the electronic and steric environment [14–16]. Polypyrrole is suitably adapted for addressable electrochemical polymerization, acting as linking agent for the immobilization of the DNA probe and insures efficient electron transfer between the relay (ferrocene moieties) and the electrode surface. These polymers satisfy all the requirements for producing high-density arrays of individually addressable DNA-functionalized microelectrodes for further integration in a chip format. With this aim, we report in this work, the integration of the copolymers 1-(phthalimidylbutanoate)-1′-(N-(3-butylpyrrole)butanamide)ferrocene, and pyrrole into a chip format by grafting various DNA probes in high-density arrays of individually addressable oligonucleotide microelectrodes. We demonstrate that the effect of reducing the size of the electrodes

* Corresponding author. Tel.: +33 1 69 15 74 40; fax: +33 1 69 15 72 81.
E-mail address: hafsa.korri-youssoufi@u-psud.fr (H. Korri-Youssoufi).

0039-9140/$ – see front matter © 2010 Elsevier B.V. All rights reserved.
doi:10.1016/j.talanta.2010.02.017

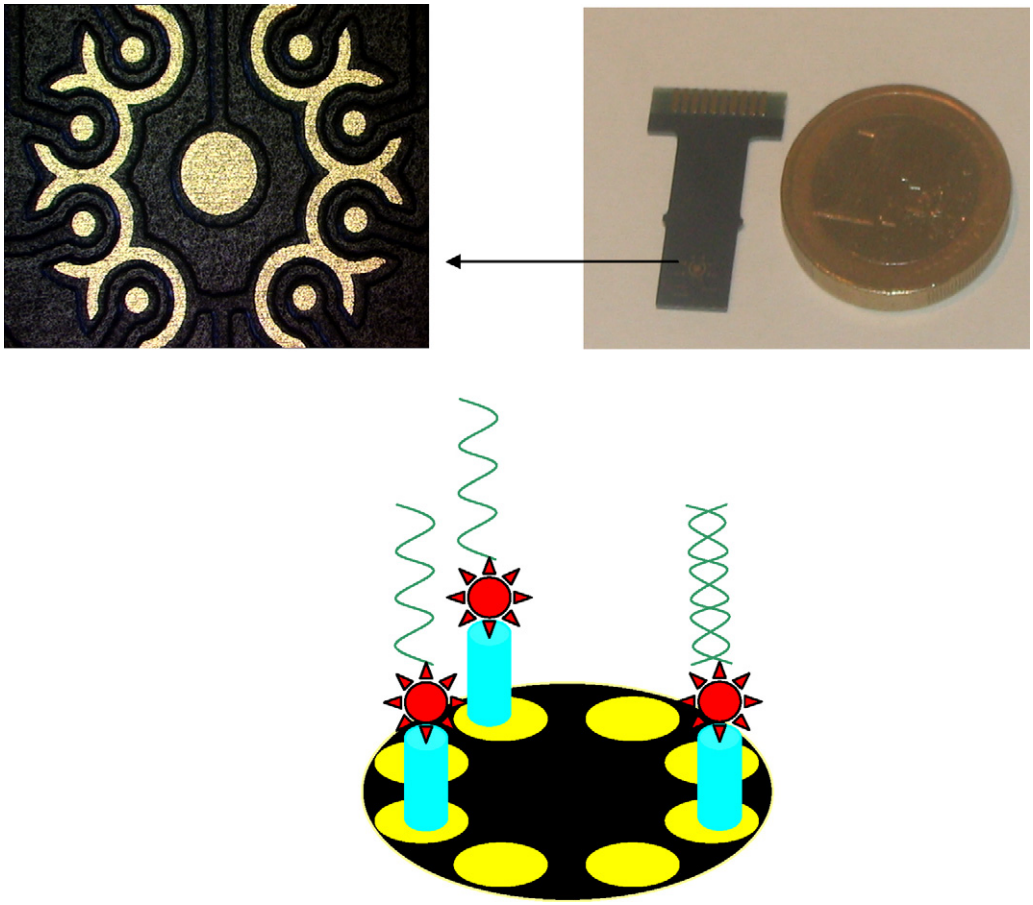

Scheme 1. Photograph of the chip employed and the scheme giving their dimensions and the procedure for multi-detection analysis.

and the geometry of the chip integration influences the sensitivity and selectivity in comparison with the macroelectrode results.

2. Materials and methods

2.1. Reagents

The ferrocene monomer, 1-(phthalimidylbutanoate)-1′-(N-(3-butylpyrrole)butanamide)ferrocene (Py-Fe-NHP) was synthesized following the procedure described previously [17], and pyrrole was distillated before use.

All the oligonucleotides (DNA) used in this work were provided by bioMérieux company. The oligonucleotide probe was a 25-mer sequence with an amino group on the 5′ phosphoryl terminus: NH_2-5′TCA-ATC-TCG-GGA-ATC-TCA-ATG-TTA-G3′. The sequence of the target oligonucleotide, complementary to the 25-mer oligonucleotide probe was: 5′CTA-ACA-TTG-AGA-TTC-CCG-AGA-TTG-A3′. The non-complementary 25-mer oligonucleotide target was: 5′TAA-AGC-CCA-GTA-AAG-TCC-CCC-ACC3′. Stock solutions of the target and non-complementary oligonucleotides at various concentrations between 0 and 0.5 nmol L^{-1} were prepared in 0.1 M phosphate buffer solution at pH 6.8 and stored in a freezer.

The grafting of ODN target was achieved by dipping the electrode in solution of DNA probe for 1 h at room temperature. Hybridization was realized by contact of the sensor surface with a solution of DNA target for 2 h. For fluorescence measurement on the chip, hybridization of 5′ biotinylated DNA target was realized in the same conditions as above. This step is followed by a conjugated step, where a solution of 20 μM streptavidin-R-phycoerythrine was incubated with the chip during 30 min. After washing, the fluorescence was measured with fluorescence microscope (BX, Olympus) equipped with CDD camera.

2.2. DNA chips

The chips were provided by bioMérieux. They constituted of 10 gold electrodes constructed by printed circuit board technology (Scheme 1). The reference electrode and the auxiliary electrode were integrated in the chip design. The analysis area of the chip consists of 8 circular 200 μm diameter working electrodes surrounded by a reference electrode and a 600 μm diameter auxiliary electrode in the center of the chip.

2.3. Electrochemical measurements

Electrochemical experiments were performed with a computer-controlled potentiostat BioLogic from Sciences Instruments. Cyclic voltammetry analysis was performed in 10 mM PBS solution after each step of the construction of the biosensor. The ferrocene redox couple potential was measured for both electrochemical cells in macroelectrode and chip format and all the measured potentials were referenced versus the redox potential of the ferrocene redox couple.

2.4. Electropolymerization

Electrochemical polymerization on a macroelectrode was performed in a one-compartment cell. A three-electrode system comprising a gold disk as working electrode with an area of 3.14×10^{-2} cm^2, a platinum mesh as counter electrode and a satu-

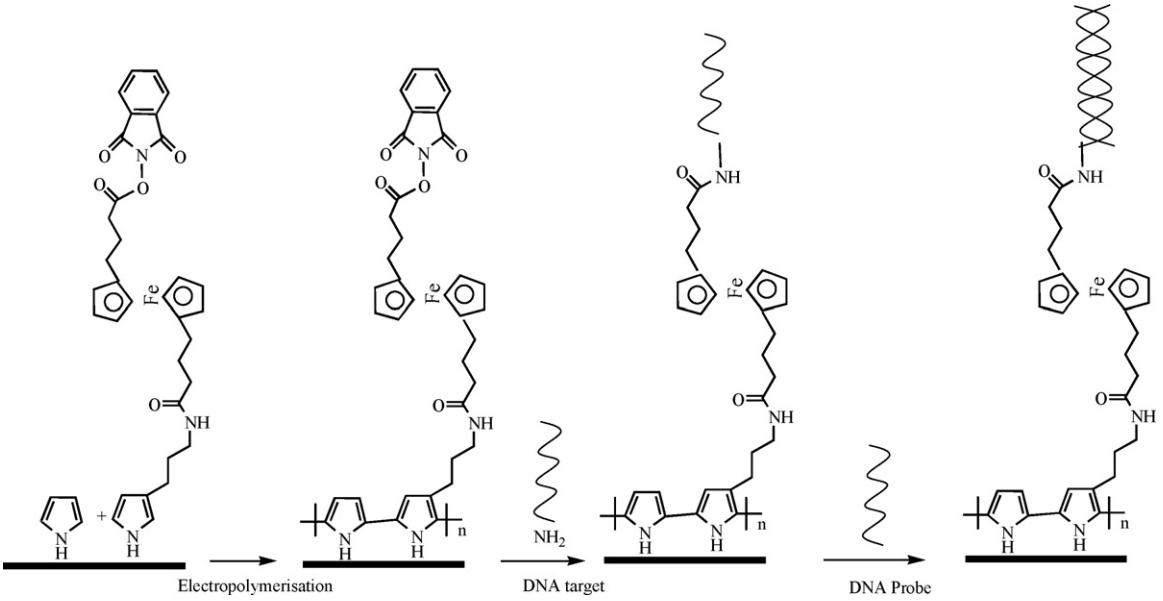

Scheme 2. Synthetic strategy for the construction of the biosensors by electrochemical copolymerization reaction followed by covalent attachment of DNA probe and hybridization of the DNA target.

rated calomel electrode as reference were used. In the case of the polymerization on the chip, the reference electrode used, was a bare gold electrode integrated on the chip. Before electropolymerization the solution was degassed by bubbling argon. Copolymer precursors were grown in acetonitrile solution containing a mixture of the two monomers pyrroles Py-Fe-NHP and Py in a concentration ratio 8:2 mM and 0.1 M $LiCLO_4$ in acetonitrile solution at a fixed potential of 0.8 V/ferrocene. The polymerization was halted after a measured charge corresponding to 20 mC/cm^2 was passed.

2.5. SEM measurements (SEM)

The scanning electron micrographs have been carried out with a Leica/Cambridge 260.

3. Results and discussion

Biological analysis has evolved toward miniaturization and real-time measurements; however molecular biology needs to integrate sample preparation steps with amplification and detection. Multi-detection methods are forecasted to routinely identify several targets in real-time with the appropriate controls. Our research effort considers direct electrical measurement approaches in order to simplify and shorten the time of molecular detection for nucleic acid targets. We have generated conductive polypyrrole layers on gold electrodes of printed circuit board (PCB) chips on which we have grafted the desired probe (Scheme 2). Detection measurement is based on the signal modification during a biological recognition of DNA hybridization of the ferrocene/ferrocenium redox couple which is included in a well-defined molecular architecture of polypyrrole described above [12].

The PCB chip is essentially dedicated to fast on-field analysis of chemical and biological substances in small volumes of solution. bioMérieux has developed a disposable low-cost multi-test chip to fulfil this requirement. In a typical experiment, microelectrodes with a surface area of 3.14×10^{-4} cm^2 are prepared by standard printed circuit technology. The chip consists of 8 working electrodes, an auxiliary electrode and a reference electrode. The required volume for electropolymerization and DNA immobilization is less than 50 μL.

3.1. Effect of reducing the electrode size on electropolymerization reaction

The size of the electrode and the architecture of the electrochemical cell have a large effect on the kinetics of the electropolymerization reaction. Fig. 1 shows the current–time transient measurement during the polymerization process on macroelectrode and chips. The current–time transient of the polymerization on the macroelectrode (Fig. 1a) shows an increase of current during the first step, followed by the decrease of current and then stabilisation during the growth of the polypyrrole films. However the polymerization reaction occurring on the chip (Fig. 1b) shows an increase of current during all processes of the polymerization as well as for the film growth.

It can also be noticed that the polymerization time on the chip took 1.6 s compared to 30 s for the macroelectrode for the same density of charge. These differences underline that the kinetics of the polymerization reaction obtained on a chip are different from the macroelectrode and could influence the structure and morphology of the obtained polypyrrole film.

To explain the origin of the variation of the electropolymerization and growth of the polypyrrole layers between the chips format and macroelectrode, we will serve of the model established by Harrison and Thirsk [18]. It has been demonstrated previously that the polymerization of the polypyrrole layer follows the various mechanisms of nucleation and growth established in this model [19,20] and the morphology of the polypyrrole film was depending of the mechanism of electropolymerization process.

The model demonstrates that, there are two kinds of nucleation, namely instantaneous and progressive, and two types of growth two-dimensional (2D) and three-dimensional (3D). In the instantaneous nucleation mechanism the number of nuclei is constant and they grow in their former positions on the bare substrate without the formation of new nuclei. Hence the radii of nuclei are larger and the surface morphology is rough. In progressive nucleation, the nuclei not only grow on their former positions but also on new nuclei which form smaller particles giving an overall flatter surface morphology. For 2D growth the nuclei grow more quickly in the parallel direction than in the perpendicular direction growing laterally until they impinge on each other. However, in the 3D growth model, the nuclei growth rate is essentially equal in the parallel and

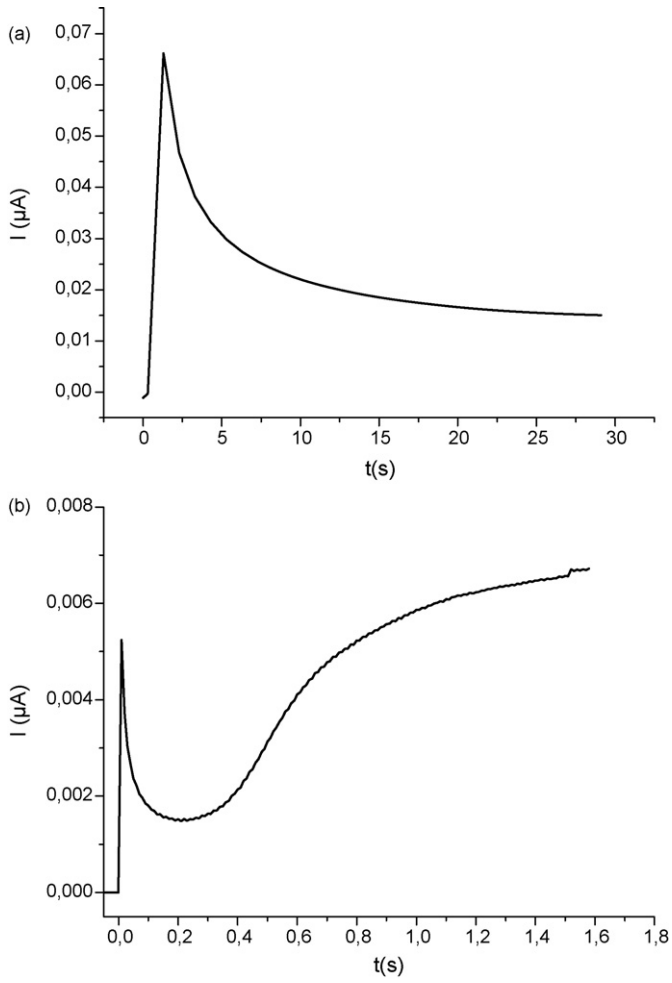

Fig. 1. Chronoamperometric curves of functionalized copoly[Py-Fe-NHP, Py] deposited on the macroelectrode and on the chip.

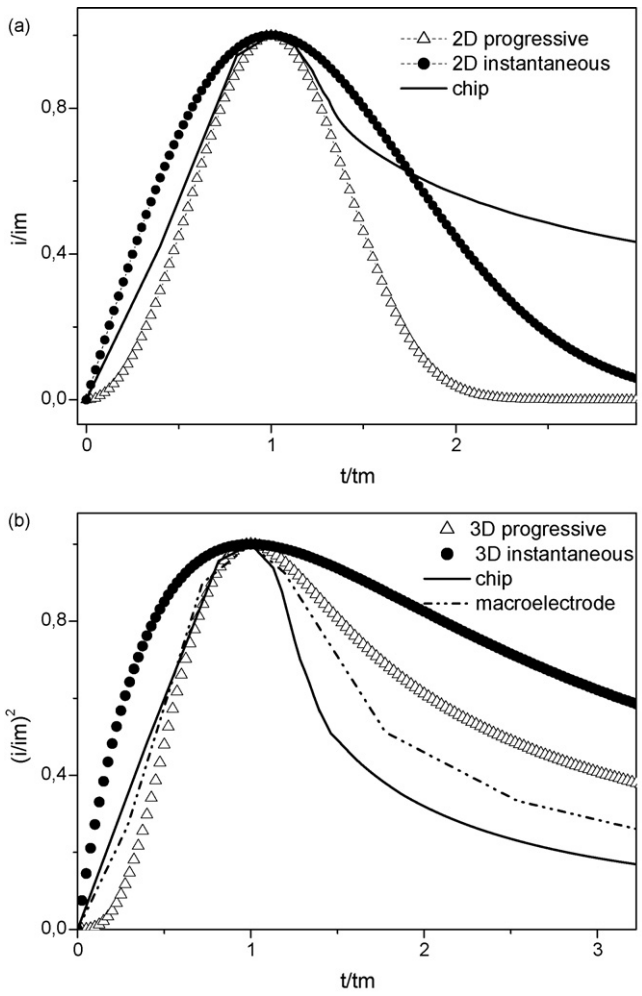

Fig. 2. Dimensionless plots of *I–t* curves for copoly[Py-Fe-NHP, Py] polymerized electrochemically on gold substrates on the macroelectrodes and on the chip electrode. compared with theoretical models for 2D and 3D instantaneous and progressive nucleation.

perpendicular directions with the respect to the electrode surface. Harrison and Thirsk show that, the shape of the current–time transient is indicative of the nucleation and the growth mechanism. Theoretical plots for progressive and instantaneous nucleation for both 2D and 3D cases are given by the following equations where the t_{max} and I_{max} are the coordinates of the time at current maximum.

2D growth progressive nucleation

$$\frac{I}{I_{max}} = \left(\frac{t}{t_{max}}\right) \exp\left(-\frac{2}{3}\frac{t^3 - t_{max}^3}{t_{max}^3}\right)$$

2D growth instantaneous nucleation

$$\frac{I}{I_{max}} = \left(\frac{t}{t_{max}}\right) \exp\left(-\frac{1}{2}\frac{t^2 - t_{max}^2}{t_{max}^2}\right)$$

3D growth progressive nucleation

$$\left(\frac{I}{I_{max}}\right)^2 = 1.2254\left(\frac{t}{t_{max}}\right)\left(1 - \exp\left(-2.3367\left(\frac{t}{t_{max}}\right)^2\right)\right)^2$$

3D growth instantaneous nucleation

$$\left(\frac{I}{I_{max}}\right)^2 = 1.9542\left(\frac{t}{t_{max}}\right)\left(1 - \exp\left(-1.2564\left(\frac{t}{t_{max}}\right)\right)\right)^2$$

The theoretical plots are fitted with the experimental data from current–time transient for the polymerization of the copoly [Py-Fe-NHP-co-Py] on both electrodes. Fig. 2a, b shows respectively the comparison of experimental data with the theoretical curves of 2D instantaneous and progressive nucleation and growth and 3D instantaneous and progressive nucleation. It is clear that the experimental curves for polypyrrole deposition on a macroelectrode show poor fitting of the 2D models. The experimental data fit more with theoretical curves of 3D instantaneous nucleation and growth. However the experimental curves for the deposition of functionalized polypyrrole on the chip coincide with 2D progressive nucleation which deviates after the nuclei overlap from whence the experimental curve better fits the 3D progressive nucleation process. These variations could be due to the geometry of the cell between the macroelectrodes and the chips and also as well as on the nature of the surface. It was demonstrated that the nature of the surface, from hydrophobic/hydrophilic character and their roughness influence the mechanism of electropolymerization of pyrrole. Hwang et al. [21] demonstrated in the case of the polymerization of pyrrole on HOPG, that by varying the nature of HOPG surface from hydrophilic to hydrophobic leads to significant modification of the mechanism. They observed that the polymerization follows a mechanism with a combination of instantaneous 2D and progressive 3D for a hydrophilic surface and 3D progressive mechanism for a hydrophobic surface. The roughness of the gold surface also has an effect on the mechanism of the electropolymerization of pyrrole. Liu and Wang [22] showed that the roughness of the

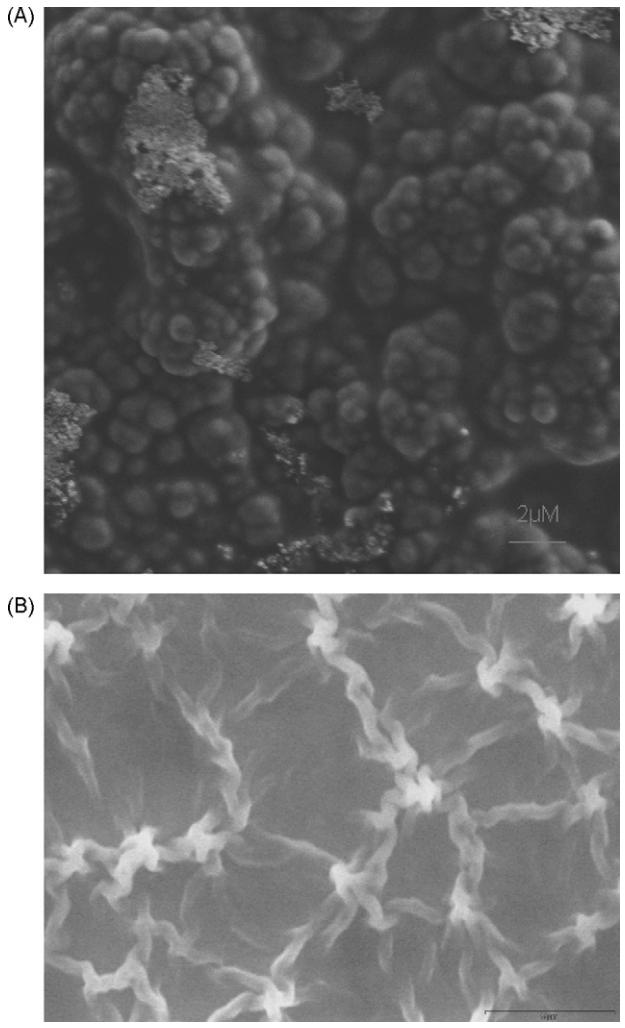

Fig. 3. SEM micrographs of copoly[Py-Fe-NHP, Py]: (a) deposited on macroelectrode and (b) deposited on chip.

gold surface influences the mechanism of the polymerization. On the gold surface modified by plasma treatment the mechanism is 3D instantaneous, however positive deviation of I/I_{max} is observed for an non-treated gold electrode.

In the case of the chip electrodes formed by PCB technique the surface is more hydrophobic than the gold macroelectrode as demonstrated by the measured contact angle. The properties of the electrode surface besides the geometry of the chip should also lead to a variation in the mechanism of the polymerization where 2D progressive nucleation is obtained in a first step followed by 3D progressive nucleation after nuclei begin to overlap. These modifications in the mechanism of polymerization lead to a variation in surface morphologies of the functionalized polypyrrole obtained on both electrodes.

The SEM images of the polypyrrole layers distinguish different morphologies between the functionalized copolypyrrole grown on the macroelectrode and the chip electrode. The polypyrrole deposited on the macroelectrode (Fig. 3a) shows a rougher and more compact morphology in concordance with the instantaneous nucleation observed generally in the case of polypyrrole [23]. The deposition of the polypyrrole on the chip format as shown in Fig. 3b exhibits a highly microporous surface morphology structure with polymer fibrils of a few microns in diameter. Such structures are due to progressive nucleation as described above. The 2D growth of the polypyrrole in the first step leads to a rapid growth of nuclei in

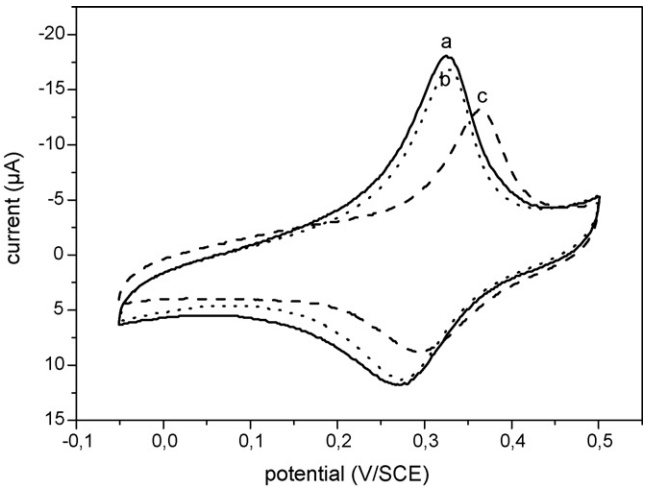

Fig. 4. Electrochemical voltammograms of copoly[Py-Fe-DNA, Py] deposited on the macroelectrode, analysed in PBS buffer solution scan rate 50 mV/s: (a) before hybridization, (b) after incubation with 200 nM of non-complementary DNA and (c) after incubation with 200 nM of complementary target DNA.

the parallel direction to form a larger nucleus, or knot, from which 3D growths continues in equal measure along parallel and perpendicular directions to the electrode surface leading to the formation of a fibril morphology. Such microporous morphology provides a larger surface area compared to the compact structure obtained on the macroelectrodes.

Various other parameters could be the origin of such variation. Firstly the geometry of the chip format has an optimized configuration in which the counter and reference electrode are a very small distance to the working electrode. Secondly the specific mass transport properties differ for the two electrode geometries; governed by a linear and radial diffusion process for the macroelectrodes and microelectrodes, respectively [24,25]. Thus, it was established that in the case of a macroelectrode the concentration of active compounds varies linearly between the bulk of sample solution and the electrode surface leading to planar diffusion. In contrast, for microelectrodes, the main concentration within the surface is comparable to the electrode radius [26] allowing spherical diffusion. In the case of polymerization reaction the steady state concentration of electroactive species (pyrrole monomer) varied from macroelectrode to microelectrode format. Such phenomena should favour the electropolymerization reaction on the microelectrode surface instead of macroelectrode.

3.2. The effect of reducing the electrode size on the electrochemical properties of the biosensors

A DNA probe bearing an amino group in its terminal position was immobilized on the copolymer by spotting 50 μL or 5 mL of solution of DNA probe on the appropriate electrode. Covalent attachment of the DNA probe by the formation of an amide link was performed by the reaction of the amino group of DNA and activated ester of the functionalized polypyrroles layer.

The electrochemical signal of the ferrocenyl group was analysed in aqueous media after each step of the construction of the biosensor, immobilization of DNA probe and hybridization reaction with non-complementary DNA and complementary DNA for both types of electrode (see Figs. 4 and 5). Both devices demonstrate a strong electroactivity and reversibility of the attached ferrocenyl group this aided by the high conductivity of the polypyrrole layers [27]. The redox potential obtained for ferrocene deposited on the macroelectrode is 0.185 V/ferrocene and 0.036 V/ferrocene for the chip format electrode. However, we observe that the electrochemical

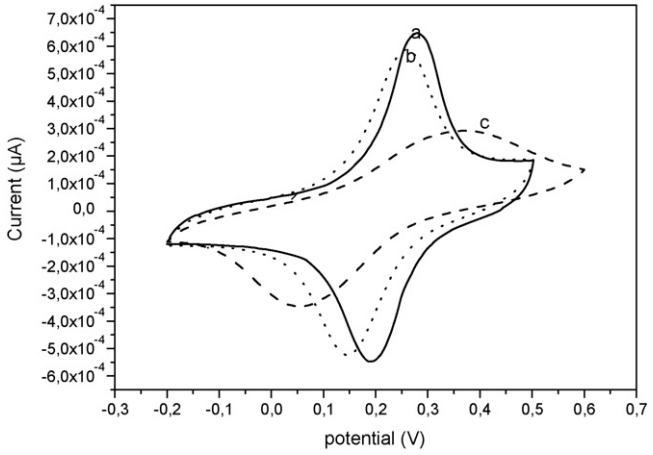

Fig. 5. Electrochemical voltammograms of copoly[Py-Fe-DNA, Py] deposited on the chip in PBS buffer solution scan rate 50 mV/s: (a) after formation of the biolayer, (b) after incubation with 200 nM of the non-complementary target and (c) after hybridization with 200 nM of the complementary DNA target.

signal obtained on the chips shows more symmetric waves of the oxidation and the reduction. Thus underlines that the electrochemical signal of the ferrocene is more reversible on the chip than for the macroelectrodes. This observation can be related to the high conductivity of the polypyrroles layer formed on the chip in which the geometry of the counter and reference electrode are optimized. The diffusion and migration processes acting at the macroelectrode and microelectrode during electrochemical measurement could also be the origin of such variation in electrochemical response. It was established for the macroelectrode that the amperometric current response depends on the thickness of the diffusion layer, however in the case of microelectrode the current is independent of the diffusion layer thickness and depends on the radius of the electrode [28].

Hybridization was performed by incubating electrodes with target DNA or non-target DNA in 50 μL or 5 mL of solution depending on the electrode. After incubation with non-complementary target in which no hybridization takes place, the electrochemical signal shows no significant variation (Figs. 4b and 5b) for both electrodes. However after incubation with complementary target (Figs. 4c and 5c) there is a large variation of electrochemical properties due to the hybridization reaction, and moreover, different variations are observed for the film on the macroelectrode and on the chip for the same concentration of DNA target. The ferrocene signal on the macroelectrode shows a small decrease of current with shift of the oxidation potential by +50 mV. For ferrocene deposited on the chip, the redox wave becomes more extended with a shift in the oxidation potential by +100 mV and hence less reversible, together with a marked decrease in the current intensity. Such a change in the current allows higher sensitivity for the chip system compared to the macroelectrode.

3.3. The effect of reducing the electrode size on the sensitivity

To check the sensitivity of the biosensor for the two types of electrode formats, the electrochemical signal of the ferrocenyl group was analysed after hybridization with various concentrations of DNA target from 0.1 to 200 nM. Hybridization induces both a shift of potential and a decrease in current depending on the concentration of DNA target in both electrodes. In the case of polymer deposited on the macroelectrode a progressive decrease in intensity besides a shift of oxidation potential is observed upon increasing the concentration of DNA target incubated. For the film deposited on the chips different variations in the signal are observed depending on

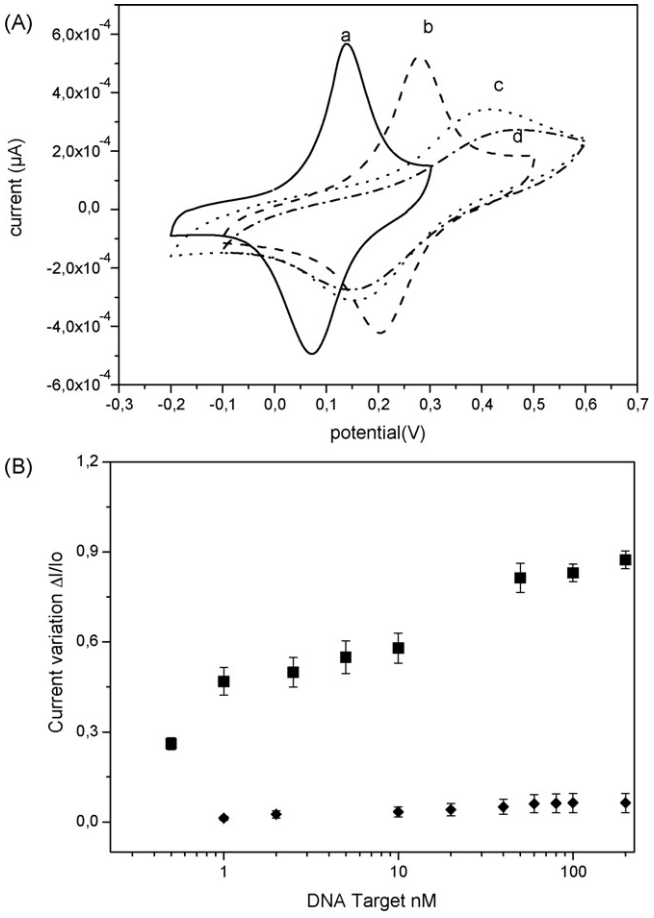

Fig. 6. (a) Voltammograms of a chip modified by copoly[Py-Fe-DNA, Py] analysed in PBS buffer solution, scan rate 50 mV/s: (a) before hybridization reaction, (b) after incubation with 0.5 fmol (10 nM) of complementary target DNA, (c) after incubation with 5 fmol (100 nM) and (d) 200 mM (10 fmol) of the complementary DNA target. (b) Calibration curve obtained by measuring the current at constant potential (♦) on the macroelectrode and (■) on the chip.

the concentration of DNA target (Fig. 6a). For small concentrations, less than 10 nM, hybridization induces a shift of the redox wave and reversibility is maintained, whilst hybridization with high concentrations (more than 50 nM) effectively breaks the signal reversibility combined with a substantial shift of the oxidation potential and decrease in the peak current.

This result can be explained as follows, the electropolymerization reaction on the chip between pyrrole bearing ferrocene and pyrrole occurs with the mechanism that favours the formation of nuclei containing fewer defects in conjugation. In this condition the polypyrroles layer is more conductive. In addition, besides the electronic conductivity of polypyrroles, redox conductivity provided from the ferrocenyl groups is also present [27]. For low concentration of DNA target, hybridization occurs only at few ferrocenyl sites, and in this case only the redox conductivity varies, whilst the electronic conductivity remains unchanged. Thus leads to a shifts of the redox signal of the ferrocenyl groups without the modification of the reversibility. Concerning incubation with a higher concentration, hybridization occurs over a large surface inducing also variation in electronic conductivity of the film. This decrease was disturbing the electron transfer from the ferrocenyl groups to the electrode via the polypyrroles layer, where in this case the change in the conductivity beside the decrease of the counter-ion mobility are being restricted by the bulky chains of DNA and their negative charge [29,30].

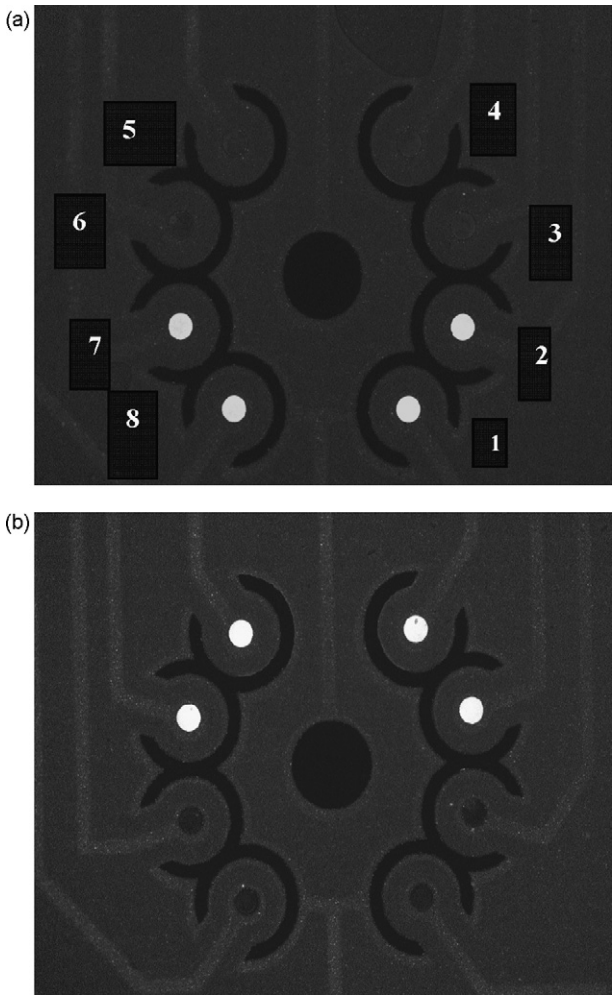

Fig. 7. Fluorescence image of the chips after hybridization with the S1-DNA target (top), and after (bottom) denaturation and hybridization with the DNA target S2.

The variation of the current intensity at constant potential of the DNA-modified electrodes after hybridization is plotted versus the concentration of incubated DNA target Fig. 6b. The detection limits were evaluated to be 1 nM (pmol) and 0.01 nM (0.05 fmol) for the macro and chip, respectively. The miniaturization has thus allowed a lower detection limit. The same behavior was also observed by Kranz's group where 27-mer oligonucleotides were immobilized on a 2,5-(-bis(2-thienyl)-N-(3-phosphoryl propyl) pyrrole film deposited on a microelectrode, allowing a detection limit of 3.5 fmol [31]. It has been demonstrated that further progress in the sensitivity and selectivity can be easily realized by reducing the size of the electrode and amount of the analyte, i.e. decreasing the DNA target [32]. In the present work the decrease of the size of the electrode and the geometry of the cell leads to a polypyrrole film with a fibril porous morphology with high surface to volume ratio, which promotes the high sensitivity in the detection.

3.4. Multi-DNA and real-time detection

To demonstrate the feasibility of multi-detection, each microelectrode was separately functionalized by spotting the appropriate capture DNA. The probe (S1) NH_2-5′TTTTTTTTTT-ATCTCGGGAATCTCAATGTTAG3′ was immobilized on electrodes 1, 2, 7, and 8. The probe (S2) NH2-5′TTTTTTTTTTTATTCC-TTGGACTCATAAGGTG3′ was immobilized on electrodes 3, 4, 5, and 6. After the immobilization procedure, the chip was washed

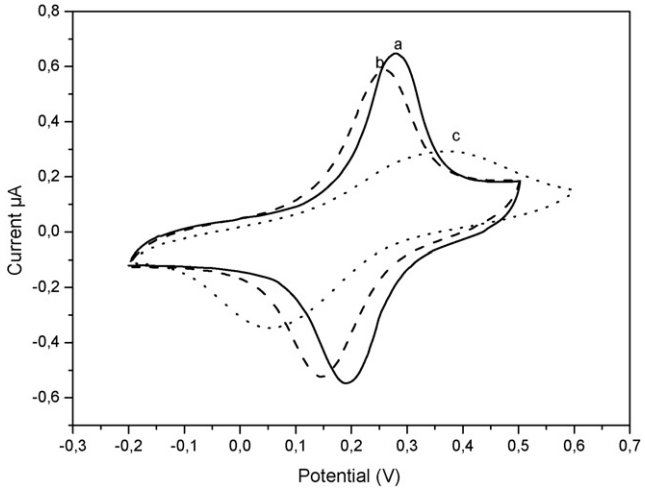

Fig. 8. Voltammograms of a chip modified by copoly[Py-Fe-DNA, Py] analysed in PBS buffer solution, scan rate 50 mV/s (a) electrodes analysed after immobilization of DNA probe S1 and S2, (b) electrodes 1, 2, 7, and 8 after incubation with 200 nM of non-complementary DNA target S2 and (c) electrodes 1, 2, 7, and 8 after incubation with 200 nM of complementary DNA target of probe S1.

to evaluate the discrimination of the complementary DNA target of probe S1 and S2 incubated with concentration of 200 nM during 2 h. In order to follow the multi-detection analysis, besides the electrochemical response, the chip array was incubated with complementary target labeled with biotin, to allow imaging, by fluorescence microscopy, the position of the hybridization by further reaction with streptavidin-phycoerythrine fluorescent dye. The fluorescence image reveals that hybridization is specific to electrodes 1, 2, 7 and 8 where the probe is complementary to the target, Fig. 7-top. The voltammetry curves show large variation of the ferrocene signal after hybridization for electrodes 1, 2, 7, and 8 (Fig. 8c). However, no electrochemical variation of the ferrocene signal was observed for electrodes 3, 4, 5, and 6 where probe S2 is expected not to form a complementary pair (Fig. 8b). Furthermore, the same chip was denaturized and then incubated with target DNA which forms a complementary pair with probe S2 and both electrochemical activity and fluorescence was checked. The voltammetry curves show the same variation as observed in Fig. 8. The fluorescence image occurs only on electrodes 3, 4, 5, and 6 (Fig. 7-bottom), which expected to form complementary pairs, whilst no responses were observed for electrodes 1, 2, 7, and 8 where the probe is not complementary to the target.

The multi-detection analysis was then performed by simultaneous hybridization of the two DNA targets present in the same solution, in this case all the electrodes show the variation in electrochemical signal as above (same as Fig. 8). Such system should offer the possibility of multi-detection analysis of 8 DNA targets as the chip was formed with 8 working electrodes individually addressable. These results show the possibility offered by this chip design for multi-detection of various DNA targets.

4. Conclusion

We have reported a type of biosensor for DNA hybridization based on a copolymer formed with pyrrole substituted with ferrocenyl groups acting as electrochemical probes, and N-hydroxyphthalimide as a leaving group to allow covalent attachment of the DNA probe onto small microelectrodes arranged in a matrix array format. The electrochemical response of the sensors was evaluated and compared to those deposited on a macroelectrode. Results show that an enhancement of the sensitivity of the detection was obtained by using a well-defined electrode (or cell)

architecture in a chip array format. The detection limit calculated in the case of the chip format is evaluated to 0.05 fmol.

Thus, by combining an electrochemical relay, the ferrocene and the conducting polymer as transducer, we have demonstrated that such system was promising in the design of high-density microelectrode arrays based on multiple probes for simultaneous detection of various DNA targets.

Acknowledgement

Bio-Mérieux Company Lyon, France, was acknowledged for materials support.

References

[1] F. Bier, M. Nickish-Rosenegk, E. Ehrentreich-Föster, E. Reib, J. Henkel, R. Strehlow, D. Andersen, Adv. Biochem. Eng. Biotechnol. 109 (2008) 433–453.
[2] J. Wang, Chem. Eur. J. 5 (1999) 1681–1685.
[3] T. Livache, H. Bazin, G. Mathis, Clin. Chim. Acta 278 (1998) 171–176.
[4] T. Livache, E. Maillard, N. Lassalle, P. Mailley, B. Corso, P. Guedon, A. Roget, Y. Levy, J. Pharm. Biomed. Anal. 32 (2003) 687–696.
[5] H. Peng, L. Zhang, C. Soeller, J. Travas-Sejdic, Biomaterials 30 (2009) 2132–2148.
[6] K. Khrishnamoorthy, R.S. Gokhale, A.Q. Contractor, A. Kumar, Chem. Commun. 7 (2004) 820–821.
[7] H. Korri-Youssoufi, A. Yassar, Biomacromolecules 2 (2001) 58–64.
[8] H. Peng, C. Soeller, N. Vigar, A.A. Kilmartin, M.B. Cannell, G.A. Bowmaker, R.P. Cooney, J. Travas-Sedjic, Biosens. Bioelectron. 20 (2005) 1821–1828.
[9] T.Y. Lee, Y.-B. Shim, Anal. Chem. 73 (2001) 5629–5632.
[10] J. Cha, J.I. Han, Y. Choi, D.S. Yoon, K.W. Oh, G. Lim, Biosens. Bioelectron. 18 (2003) 1241–1247.
[11] A. Najari, H.-A. Ho, J.-F. Gravel, P. Nobert, D. Boudreau, M. Leclerc, Anal. Chem. 78 (2006) 7896–7899.
[12] H. Korri-Youssoufi, B. Makrouf, Anal. Chim. Acta 469 (2002) 85–92.
[13] A. Bouchet, C. Chaix, C.A. Marquette, L.J. Blum, B. Mandrand, Biosens. Bioelectron. 23 (2007) 735–740.
[14] T. Ihara, Y. Maruo, S. Takenaka, M. Takagi, Nucleic Acids Res. 24 (1996) 4273–4280.
[15] M. Mizuta, T. Terada, K. Seio, M. Sekine, Nucleic Acid Symp. Ser. 48 (2004) 237–238.
[16] M. Nakayama, T. Ihara, K. Nakano, M. Maeda, Talanta 56 (2002) 857–866.
[17] H. Korri-Youssoufi, B. Makrouf, Synthetic Met. 119 (2001) 265–266.
[18] J.A. Harrison, H.R. Thirsk, in: A.J. Bard (Ed.), Electroanalytical Chemistry, vol. 5, Marcel Dekker, NY, 1971, p. 67.
[19] E. Garfias-García, M. Romero-Romo, M.T. Ramírez-Silva, J. Morales, M. Palomar-Pardavé, J. Electroanal. Chem. 613 (2008) 67–79.
[20] B.J. Hwang, R. Sanhanam, Y.L. Lin, Electrochim. Acta 46 (2001) 2843–2853.
[21] B.J. Hwang, R. Santhanam, Y.L. Lin, Electroanalysis 15 (2003) 115–120.
[22] Y.C. Liu, C.C. Wang, J. Phys. Chem. B 109 (2005) 5779–5782.
[23] S. Carquigny, O. Segut, B. Lakard, F. Lallemand, P. Fievet, Synthetic Met. 158 (2008) 453–461.
[24] M.I. Montenegro, M.A. Queiros, J.L. Daschbach (Eds.), Microelectrodes: Theory and Applications, Kluwer, Dordrecht, 1991.
[25] M. Fleischmann, S. Pons, D.R. Rollison, P.P. Schmidt, Ultramicroelectrodes, Datatech Systems Inc., Morgantown, NC, 1987.
[26] A.J. Bard, L.R. Faulkner, Electrochemical Methods, Fundamentals and Applications, Wiley, New York, 1980.
[27] G. Zotti, S. Zecchin, G. Schiavon, Chem. Mater. 7 (1995) 2309–2315.
[28] W.E. Morf, Anal. Chim. Acta 330 (1996) 139–149.
[29] B. Piro, S. Reisberg, V. Noel, M.C. Pham, Biosens. Bioelectron. 22 (2007) 3126–3131.
[30] C. Tlili, H. Korri-Youssoufi, L. Ponsonnet, C. Martelet, N. Jaffrezic-Renault, Talanta 68 (2005) 131–137.
[31] C.S. Riccardi, H. Yamanaka, M. Josowicz, J. Kowalik, B. Mizaikoff, C. Kranz, Anal. Chem. 78 (2006) 1129–1245.
[32] S.J. Park, T.A. Taton, C.A. Mirkin, Science 295 (2002) 1503.